

## Dynamic Mechanical Properties of Oil-Extended Reinforced SBR Rubbers

T. G. ÅREDAL, *Department of Polymer Technology, Royal Institute of Technology, Stockholm, Sweden*

### Synopsis

The dynamic mechanical behavior of six samples of styrene-butadiene random copolymers (SBR with 24% styrene) containing different amounts of carbon black and oil extender has been investigated in the temperature range  $-50^{\circ}$  to  $80^{\circ}\text{C}$ . The measurements were carried out using a Fitzgerald apparatus working in the frequency range of 0.1 to 1.0 kHz. Master curves for all materials were obtained by the method of reduced variables. The master curves show that increasing amounts of carbon black in SBR increase both the elastic ( $G'$ ) and the viscous ( $G''$ ) components of the complex shear modulus. The loss factor ( $\tan \delta$ ) decreases markedly with increasing amounts of carbon black. Increasing amounts of oil extender increase the loss factor within the reduced frequency range here reported ( $2 < \log \omega a_T < 7$ ).

### INTRODUCTION

It is well known that SBR rubbers with different dynamic mechanical properties can be produced by varying the composition and structure of the material.

Various methods of moving the transition region to a desired temperature range are known. For SBR rubber, the transition region can be displaced within the range from about  $-100^{\circ}$  to about  $100^{\circ}\text{C}$  by varying the ratio of styrene to butadiene.<sup>1-5</sup> Another method of displacing the transition region is to incorporate plasticizers such as different types of oil.<sup>6-11</sup> The height and width of a transition peak can be varied by incorporating different amounts of filler<sup>6-11</sup> such as carbon black, graphite, talc, asbestos, or mica into the rubber.

The aim of this study has been to obtain information concerning the dynamic mechanical behavior of the well-known rubber SBR 1500 by varying the amount of carbon black and oil, and to compare the results obtained with those published earlier for such systems.

### EXPERIMENTAL

Six different SBR vulcanizates based on a copolymer of styrene and butadiene (SBR) with 24% styrene, but containing different quantities of carbon black and oil, have been studied. Their formulations are given

TABLE I  
Formulations of the Experimental Materials

Material no.	1	2	3	4	5	6
SBR 1500	100	100	100	100	100	100
Carbon black (HAF-ISAF)	25	50	50	50	80	80
Extender	10	10	30	50	10	30
Zink oxide	4	4	4	4	4	4
Stearic acid	2	2	2	2	2	2
Santocure <sup>a</sup>	1	1	1	1	1	1
TMTM	0.5	0.5	0.5	0.5	0.5	0.5
Sulfur	2	2	2	2	2	2

<sup>a</sup> Cyclohexylbenzothiazole sulfenamide.

TABLE II  
Physical and Tensile Properties of the Experimental Materials

Material no.	1	2	3	4	5	6
Hardness Shore A	53	68	58	49	80	72
Carbon black, phr	25	50	50	50	80	80
Oil, phr	10	10	30	50	10	30
Ultimate elongation, %	450	400	500	650	250	320
Tensile strength, N/cm <sup>2</sup>	971	2206	1785	1667	2256	1893
Tear resistance, N/cm	232	616	580	476	612	668
$T_g$ (dilatometer), °C	-42	-44	-41	-41	-44	-47
$T_g$ (DSC), °C	-46	-47	-47	-46	-47	-47

in Table I. The carbon black-reinforcing type lies between HAF and ISAF, with a particle size<sup>12</sup> between 17.5 and 35 nm and a density of 1800 kg/m<sup>3</sup>.

The plasticizer consists of a highly aromatic oil (Nysolvex 125) with a freezing point of about 10°C. The cure system consists of a N-cyclohexyl-2-benzothiazole sulfenamide (CBS) sulfur system and the accelerator tetramethylthiuram monosulfide (TMTM).

The amount of free sulfur remaining in the samples after vulcanization was about 0.03%. The SBR vulcanizates were aged at room temperature for at least three months after vulcanization. Their tensile properties and glass transition temperatures are listed in Table II. In the subsequent discussion of the experimental results, these samples are designated by their hardness values, e.g., material no. 1 is designated SBR 53.

Circular samples were cut with diameter and thickness varying between 10 and 19 mm and between 3 and 5 mm, respectively. Measurements were carried out in a Fitzgerald apparatus<sup>13</sup> of the transducer type which measures the complex shear modulus (or compliance)

$$G^* = G' + iG''$$

$$\tan \delta = G''/G'$$

In this apparatus, a pair of polymer samples are fitted by means of a floating mass to an aluminum cylinder on which two coils are mounted. These coils move in a magnetic field and convert mechanical force into electrical current and mechanical displacement into electrical voltage. The forces and deformations in the polymers can be calculated from the electrical resistance and reactance of these moving coils. The initial compression of the samples by the floating mass wedge structure was about 5%.

The available temperature range is from  $-50^{\circ}$  to  $150^{\circ}\text{C}$ , and the frequency can be varied continuously between 0.1 and 1.0 kHz. Each of the samples was studied at 13 different frequencies and 10 different temperatures within the frequency and temperature ranges mentioned above. The reproducibility of the results was assessed by repeat measurements on unused samples from the same batch. The deviation of the results for the modulus at room temperature was about 10%. A computer program was constructed to calculate the viscoelastic functions and to produce master curves.

## RESULTS

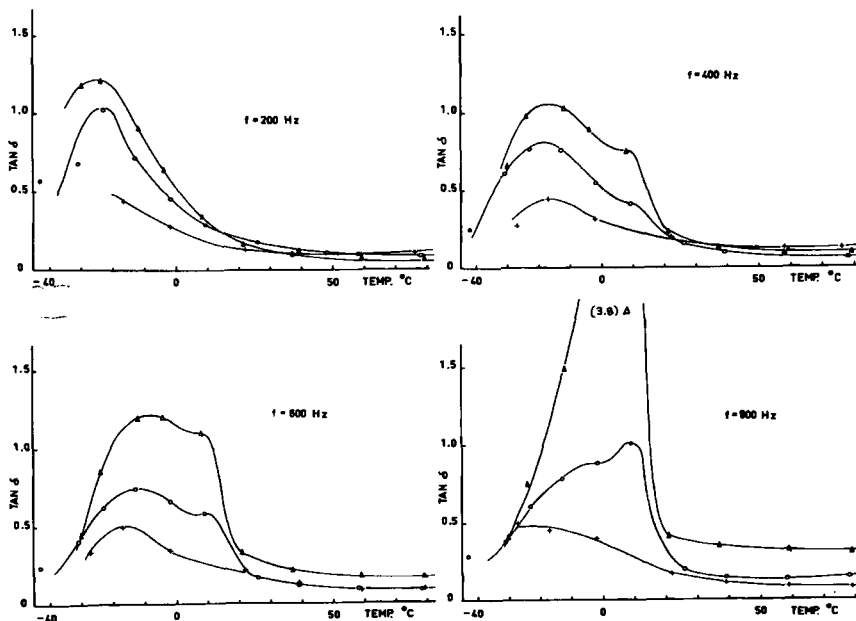
### Loss Factor

Figures 1-4 show the variation of the loss factor,  $\tan \delta$ , with temperature for three vulcanizates having different carbon black contents and a constant oil content at frequencies of 200, 400, 600, and 800 Hz. At all frequencies, increasing amounts of carbon black progressively reduce the level of the loss factor in the transition region between about  $-40^{\circ}$  and  $20^{\circ}\text{C}$ .

Increasing carbon black content leads to a decrease in the loss factor in the rubber-elastic range between about  $20^{\circ}$  and  $80^{\circ}\text{C}$  only at frequencies of 600 Hz and above. At 800 Hz, the loss factor decreases more strongly with increasing carbon black content in the whole temperature range from  $-40^{\circ}$  to  $80^{\circ}\text{C}$  than at the lower frequencies. In these figures another transition peak appears at about  $10^{\circ}\text{C}$ , which coincides with the freezing point of the oil.

With increasing frequency at a given content of carbon black, there is a broadening of the transition region. Figure 5 shows the loss factor,  $\tan \delta$ , at different frequencies for SBR 53, the material with the lowest carbon black content. The transition peak is broadened and moves from about  $-26^{\circ}$  to  $5^{\circ}\text{C}$  with increasing frequency between 200 and 800 Hz. At 800 Hz at this carbon black content, there is a very strong increase in  $\tan \delta$  in the transition range.

Figures 6-9 show  $\tan \delta$  for three vulcanizates with different oil contents and constant carbon black content at the frequencies 200, 400, 600, and 800 Hz. The loss factor  $\tan \delta$  increases slightly with increasing oil content at these frequencies, except at 800 Hz, over the temperature range from



Figs. 1-4. Variation of loss factor with carbon black content: ( $\Delta$ ) SBR 53 (25 phr carbon, 10 phr oil); ( $\circ$ ) SBR 68 (50 phr carbon, 10 phr oil); ( $+$ ) SBR 80 (80 phr carbon, 10 phr oil).

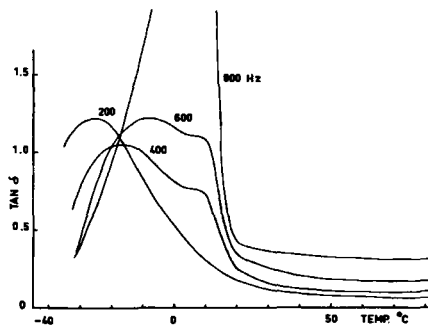
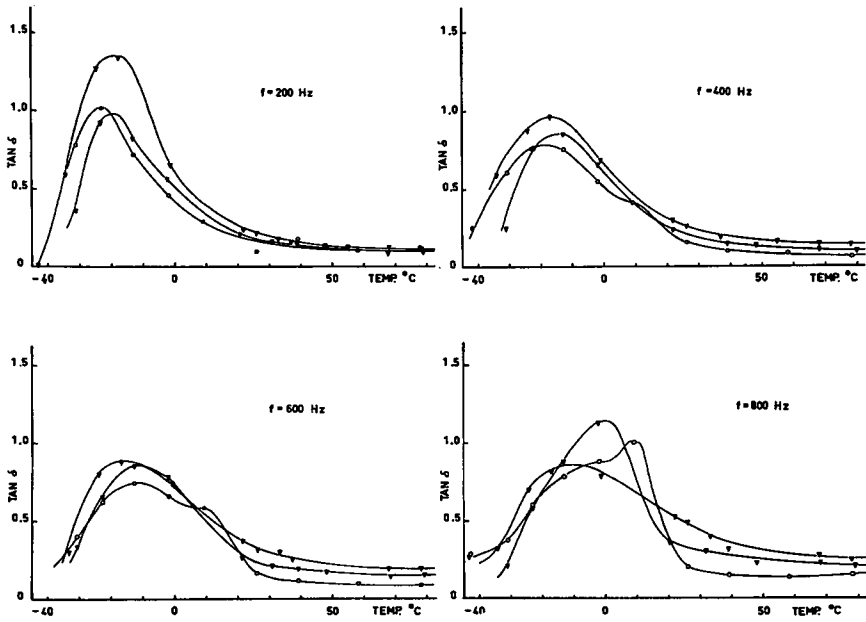


Fig. 5. Variation of loss factor with frequency for SBR 53 (25 phr carbon, 10 phr oil).

$-20^{\circ}$  to  $80^{\circ}\text{C}$ . In the rubber-elastic range, the strongest increase in  $\tan \delta$  with increasing oil content occurs at the highest frequency, 800 Hz. Figure 10 shows  $\tan \delta$  for different frequencies within the experimental temperature range for SBR 49. The transition peak is lowered and broadened and moves to higher temperatures as the frequency is increased. The curves in Figure 10 seem to intersect at a temperature of about  $-5^{\circ}\text{C}$ .

#### Master Curves from Experimental Data

In the calculation of master curves for the viscoelastic functions  $G'$  and  $G''$ , the vertical shift was taken into consideration.  $G'$  and  $G''$  have



Figs. 6-9. Variation of loss factor with oil content: (○) SBR 68 (50 phr carbon, 10 phr oil); (▼) SBR 58 (50 phr carbon, 30 phr oil); (▽) SBR 49 (50 phr carbon, 50 phr oil).

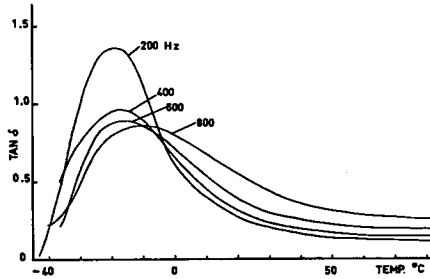


Fig. 10. Variation of loss factor with frequency for SBR 49 (50 phr carbon, 50 phr oil).

been reduced to  $G'_r$  and  $G''_r$ , at the reference temperature by the following transformations:

$$G'_r = G' \frac{T_0 \rho_0}{T \rho}$$

$$G''_r = G'' \frac{T_0 \rho_0}{T \rho}$$

where  $\rho$  and  $\rho_0$  are the densities at the temperatures  $T$  and  $T_0$ , respectively. The variation in the density with the temperature is in practice so small that  $\rho_0/\rho$  can be taken as unity.

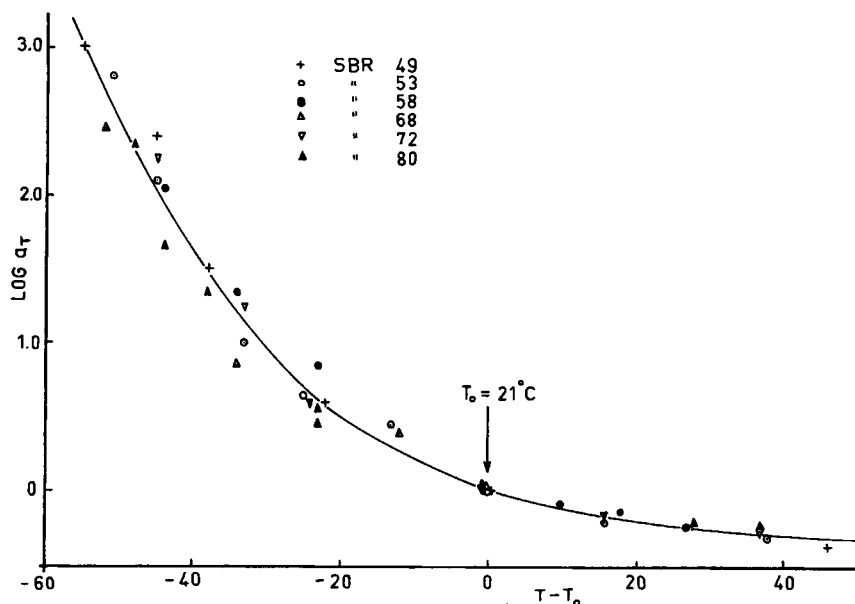


Fig. 11. Shift  $\log a_T$  for viscous part of the complex shear modulus vs. temperature.

In work of this type with thermorheologically complex materials, it is not possible to determine the horizontal shift<sup>14</sup>  $\Delta \log a_T$  by making a single shift. The shift was here determined by calculating the horizontal displacement  $\Delta \log a_T$  between each isotherm and its adjacent isotherm at three different frequencies. The average of these three shift terms was then used to construct the master curves. Where necessary, further small corrections were made in order to obtain the best fit of the data to the master curves.

When constructing the master curves, it was found that the uncertainty in  $\Delta \log a_T$  increases with increasing content of carbon black and oil. The uncertainty in the horizontal shift was estimated to be about 20%. The master curves show, however, that it is possible to produce master curves to compare different complex materials. When using the master curves for calculation and comparison, it is important that the shift for the different materials be made at about the same reference temperature  $T_0$ . In the present work, all results are referred to  $T_0 = 21^\circ\text{C}$ .

Figure 11 shows the values for  $\log a_T$  for the viscous component of the complex shear modulus plotted against  $T - T_0$  for the six materials. As is characteristic for a large number of polymers,<sup>15</sup> these values fall close to a single curve. The deviation about this curve is due to the uncertainty in the horizontal shift  $\log a_T$ .

Figure 12 shows that it is difficult to represent the behavior of these complex materials by a single WLF equation valid over the whole temperature range. In this figure, mean values have been taken from the curve of Figure 11, and  $(T - T_0)/\log a_T$  has been plotted against  $(T - T_0)$ .

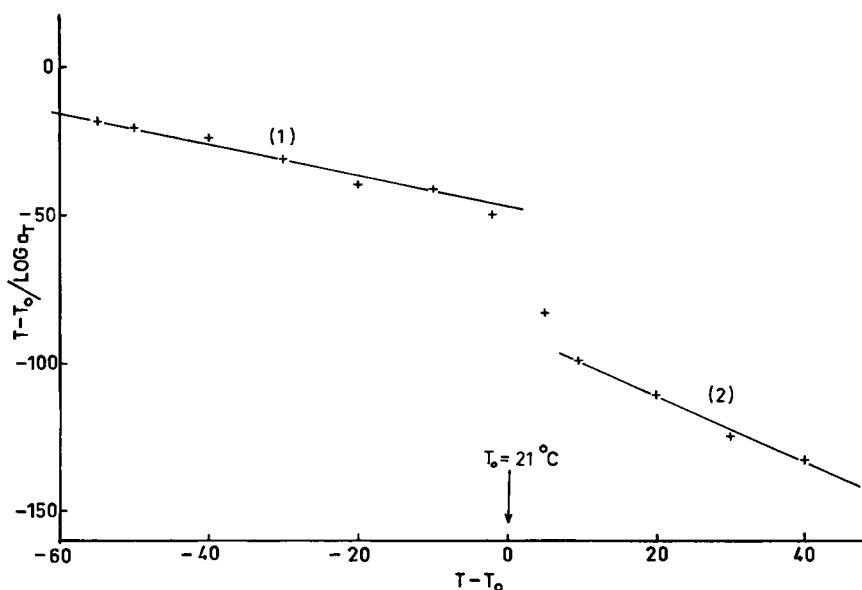


Fig. 12. WLF curves from Fig. 11.

The figure shows that the data can best be fitted to two WLF equations valid over two different temperature ranges, i.e.,

$$(\log a_T)_1 = -1.92 (T - T_0) / (90.4 + T - T_0) \quad \text{where } -60 < T - T_0 < 0$$

$$(\log a_T)_2 = -0.91 (T - T_0) / (80.9 + T - T_0) \quad \text{where } 0 < T - T_0 < 50$$

The discontinuity in Figure 12, which occurs near room temperature, is assumed to depend on the oil in the material. The oil has, as mentioned before, a freezing point of about  $10^\circ\text{C}$ , as is apparent from differential scanning calorimeter measurements as well as in the information provided by the manufacturer. The plasticizing effect of the oil, which occurs at about  $10^\circ\text{C}$  and above, causes a lower activation energy than is found in the absence of plasticizer in the material. The activation energy  $\Delta H_a$  can be calculated from the WLF equation<sup>16</sup>:

$$\Delta H_a = 2.303 R c_1 c_2 T^2 / (c_2 + T - T_0)^2.$$

Table III shows some calculated values of  $\Delta H_a$  at different temperatures. The values in parentheses are extrapolated from the lower-temperature WLF eq. (1) in Figure 12.

### Elastic Component $G'$ of Complex Shear Modulus

Figure 13 shows for comparison the master curves of the elastic modulus  $G'$  for the six different materials at the reference temperature of  $21^\circ\text{C}$ . The figures in parentheses indicate the carbon and oil contents of the ma-

TABLE III  
Activation Energies at Different Temperatures

$T, ^\circ\text{C}$	$T - T_0, ^\circ\text{C}$	$\Delta H_a, \text{kcal/mole}$
-43 ( $T_0$ )	-64	60
-39	-60	47
-20	-41	20
11	-10	10
31	10	3.8 (7.3)
61	40	2.6 (6.1)

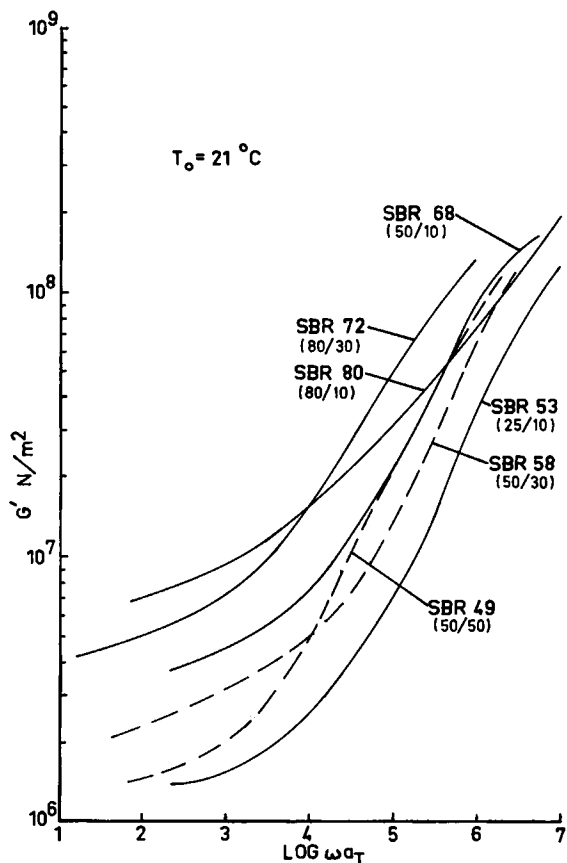


Fig. 13. Reduced master curves of elastic modulus  $G'$  for the six samples.

terials. The elastic component increases with increasing carbon black content within the frequency range  $2 < \log \omega a_T < 6$ .

A comparison of SBR 58 (50 phr carbon and 30 phr oil) with SBR 68 (50 phr carbon and 10 phr oil) shows that the elastic modulus  $G'$  decreases over the whole frequency range with increasing oil content. SBR 49, which has the highest content of oil (50 phr carbon and 50 phr oil), exhibits lower



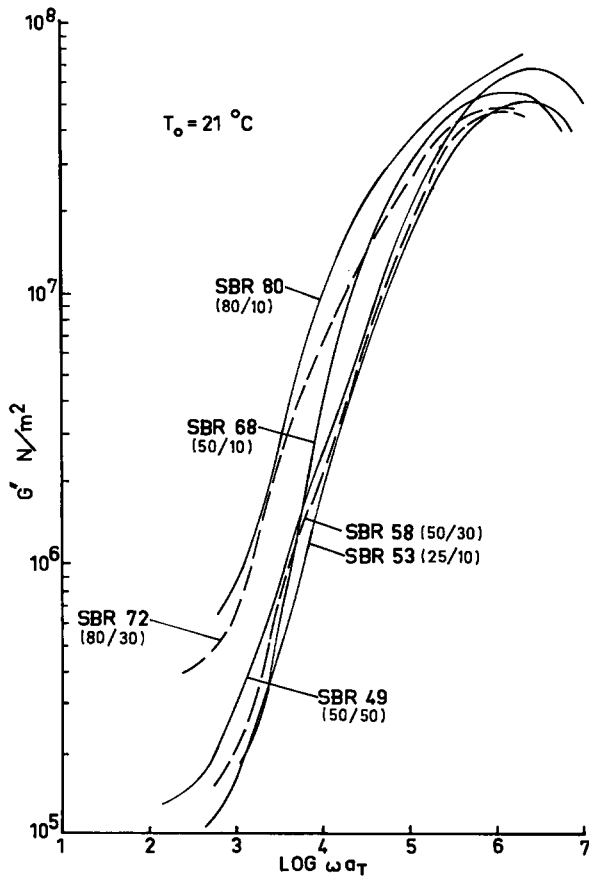


Fig. 14. Reduced master curves of loss modulus  $G''$  for the six samples.

values than SBR 58 and SBR 68 when  $\log \omega a_T < 4$ . Above this frequency, the values for SBR 49 are almost the same as those for SBR 68.

### Viscous Component $G''$ of Complex Shear Modulus

Figure 14 shows master curves of the loss modulus  $G''$  for the six different materials. Increasing content of carbon black here gives an increase in  $G''$  over the whole frequency range  $3 < \log \omega a_T < 6.5$ . That means that the energy losses in the materials increase with increasing carbon black content. The energy losses in the materials seem to decrease with increasing oil content except that SBR 49 (50 phr carbon and 50 phr oil) shows slightly higher values than the material with the lower oil content, SBR 58 (50 phr carbon and 30 phr oil).

### Loss Factor

Figure 15 compares master curves of the loss factor  $\tan \delta$  for all six materials. It is evident that the peak value of the loss factor decreases con-

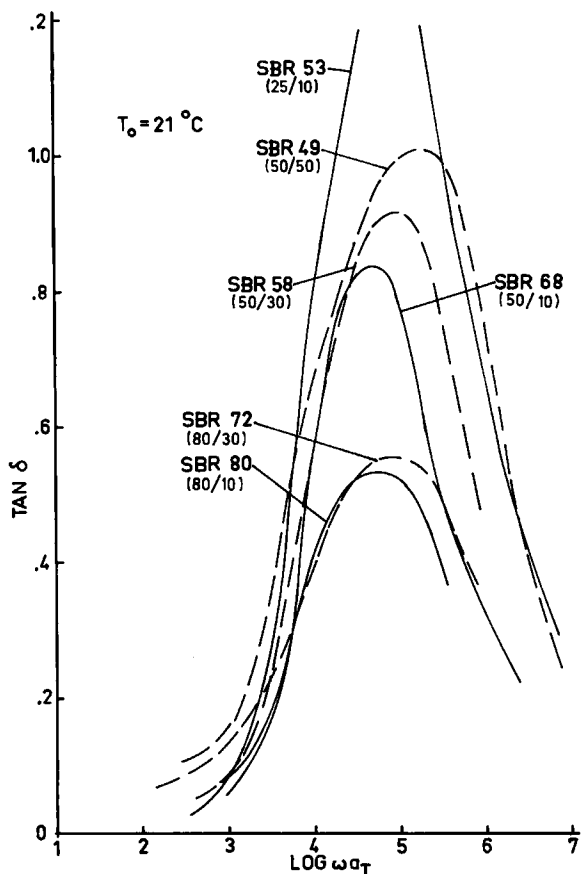


Fig. 15. Reduced master curves of loss factor for the six samples.

siderably with increasing carbon black content, but that there is virtually no displacement of the peak along the frequency axis.

With increasing oil content, the value of the loss factor is increased and at the same time the transition peak is broadened and displaced toward higher frequencies. The peak value of the loss factor lies close to  $\log \omega a_T = 5$ , which corresponds to a frequency of about 16 kHz.

## DISCUSSION

The shear amplitude for the six materials is within  $2 \times 10^{-6}$  to  $5 \times 10^{-5}$  radians, i.e., within the linear viscoelastic range. The transition region for the six materials falls between  $-40^\circ$  and  $20^\circ\text{C}$ . The glass transition temperature  $T_g$  is between  $-41^\circ$  and  $-46^\circ\text{C}$ . It has not been possible to establish any connection between  $T_g$  and the composition of the materials. The  $T_g$  was measured by a length dilatometer and a differential scanning calorimeter (DSC). The plasticizer in the materials is assumed to be the

reason for the two different WLF equations because the freezing point of the oil coincides with the temperature where the discontinuity appears in the WLF equation. This will be penetrated more in the next investigation. A study of the master curves for the loss factor  $\tan \delta$  shows that the height of the transition peak is much more affected by the content of carbon black than by the content of plasticizer. It is also evident that the position of the transition maximum on both frequency and temperature scales is not appreciably affected by the carbon black content. This has also been observed in earlier investigations. At 21°C an increasing amount of plasticizer increases the loss factor, broadens the transition range and displaces the maximum from about 8 kHz to 25 kHz.

This investigation has been supported by a grant from the Research Institute of the Swedish National Defence (FOA).

### References

1. D. D. Dunnom and H. K. de Decker, *Rubber Age* (New York), **97**, 856 (1965).
2. R. Zelenski and C. W. Childers, *Rubber Chem. Technol.*, **41**, 161 (1968).
3. K. Fujimoto and N. Yoshimura, *Rubber Chem. Technol.*, **41**, 1109 (1968).
4. K. Fujino, I. Furuta, S. Kawabata, and H. Kawai, *J. Soc. Mater. Sci. (Japan)*, **13**, 404 (1964).
5. K. Fujimoto and N. Yoshimiya, *Rubber Chem. Technol.*, **41**, 669 (1968).
6. D. A. Mayer and J. G. Sommer, *Rubber Chem. Technol.*, **44**, 258 (1971).
7. A. R. Payne, *Rubber Chem. Technol.*, **37**, 1190 (1964).
8. L. E. Nielsen, *Appl. Polym. Symp.*, **12**, 249 (1969).
9. H. K. de Decker and D. J. Sabatine, *Rubber Age*, **99**, 73 (1967).
10. G. L. Ball, *J. Acoust. Soc. Amer.*, **39**, 663 (1966).
11. P. P. A. Smit, *Rheol. Acta*, **B5**, 277 (1966).
12. G. Kraus, *Reinforcement of Elastomers*, Wiley, New York, 1965.
13. E. R. Fitzgerald and J. D. Ferry, *J. Colloid Sci.*, **8**, 1 (1953).
14. D. G. Fesko and N. W. Tschoegl, *J. Polym. Sci. C*, **35**, 51 (1971).
15. M. L. Williams, *J. Phys. Chem.*, **59**, 95 (1955).
16. J. D. Ferry, *Viscoelastic Properties of Polymers*, 2nd ed., Wiley, New York, 1970.

Received February 6, 1973